Rocturb User's Guide

Bono Wasistho

Center for Simulation of Advanced Rockets
University of Illinois at Urbana-Champaign, Urbana, IL 61801

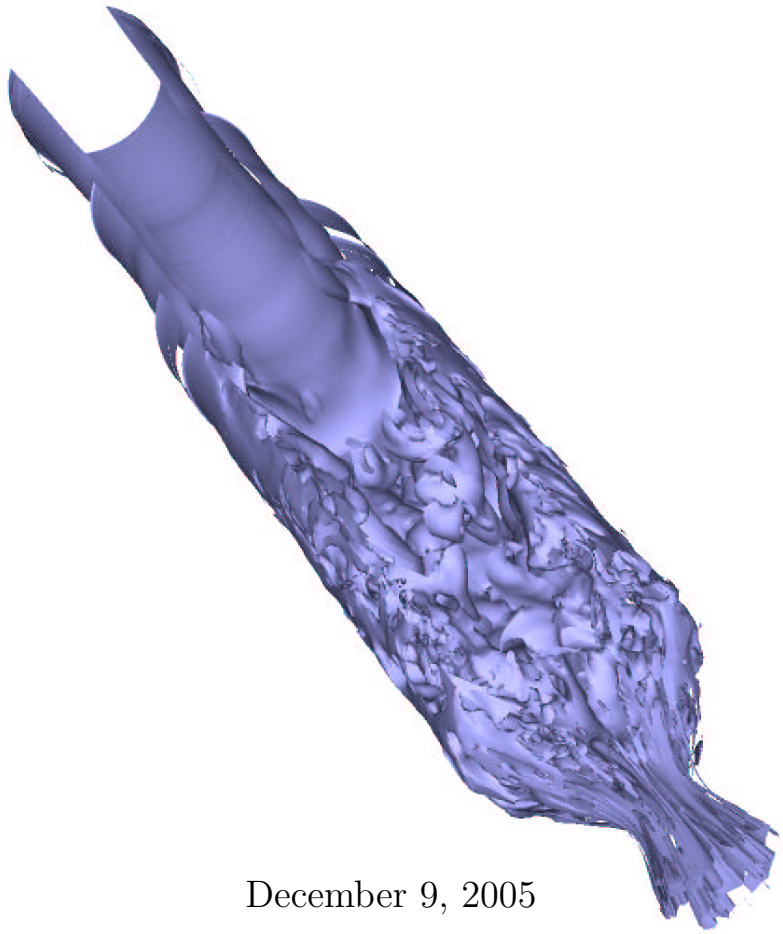

December 9, 2005

Title:	ROCTURB User's Guide
Author:	Bono Wasistho (research scientist)
Subject:	Guide for using turbulence and statistics module in Rocfluid_MP
Revision:	1
Revision history:	Revision 0: User's guide for old Rocflo code Revision 1: User's guide for Rocfluid_MP and Rocstar2.5 code Revision 2: User's guide for current Rocfluid_MP and Rocstar3 code
Effective date:	12/12/2005

Contents

Chapter 1

Introduction

1.1 Objectives

For computations involving turbulence, direct simulations of pure 3D Navier-Stokes equations in RocfloMP would in many cases be prohibitive due to high resolution requirement. This requirement can be substantially eased with the help of turbulence model because the small scale fluctuations do not have to be resolved, instead they are modeled in terms of the resolved scales on a coarser grid. This Rocturb module is therefore developed in order to provide users with various turbulence models to suit their flow features.

1.2 Model Classes and Application Regimes

We offer users three different classes of turbulence models: full LES (Large Eddy Simulation), RANS (Reynolds Averaged Navier Stokes) and Hybrid model, i.e. LES with near wall model. The near wall model can be based on Rans or turbulent boundary layer profiles in equilibrium or non-equilibrium, depending on the flow pressure gradient. For turbulent flows with thin wall shear layer, one can use LES with wall model, or DES (Detached Eddy Simulation) where the inner and outer layer is more tightly coupled. For a highly unsteady large structure motions away from the wall, such as in wall injection flows, it is recommended to use full LES as the wall requirement is less stringent, while for high Reynolds number flows with weak unsteadiness in the mean and if the interest is mainly on the mean flow, Rans is more suitable due to the less demanding grid requirement. If desired, DES can be used for high Reynolds number flow as well. DES is especially suitable for flows involving massive separation.

1.3 Reference Models Implemented

A) LES class:
1) basic Smagorinsky (Smagorinsky 1963),

2) scale-similarity (Bardina *et al.* 1984),
3) dynamic Smagorinsky (Germano *et al.* 1991 and Germano 1992),
4) dynamic mixed (Zang *et al.* 1993 and Vreman *et al.* 1994).

B) RaNS class:
1) SA (Spalart & Allmaras 1994),
2) $k - \epsilon$ (Jones & Launder 1972 and Launder & Sharma 1974).

C) Hybrid class:
1) DES (Dettached Eddy Simulation) (Nikitin *et al.* 2000),
2) Non-equilibrium wall layer model for LES (developed by Wasistho).

It is possible to select different models in different zones (zonal modeling). For instance, one can compute LES using a dynamic model in the propellant chamber, but employing the fixed Smagorinsky model in the nozzle to provide more damping along the thin boundary layer (fixed Smagorinsky without Van Driest damping provides finite, non-zero eddy viscosity at the wall)

1.4 Building and Running

To include turbulence module when creating the executable, user has to compile and link subroutines in directory *rocturb*. This is done automatically by adding option ROCTURB=1 after the compilation command *gmake* or *make* in the main directory *RocfluidMP*. To activate statistics module add STATS=1. As example, to compile with the structured grid code, one can choose following option: 'gmake RFLO=1 TURB=1 STATS=1 MPI=1'. The executable, i.e. *rflomp* for RFLO or *rflump* for RFLU, is then created in directory *RocfluidMP*. The sample input files as outlined below in Chapter Examples and Test Problems can be found in directory Rocstar/RocfluidMP/Data/. A brief explanation of regarding each input parameter and what the user is expected to enter is provided at the right hand side.

Chapter 2

Rocturb I/O Files

2.1 Input Files

2.1.1 [*CaseName*].inp file

```
# TURBULENCE
BLOCK  0  0        ! applies to block ... (0 0 = to all)
TURBMODEL  0       ! 0=laminar 1=FixSmag 2=ScalSim 3=DynSmag 4=DynMixed
                   ! 5=RaNS-SA 6=DES-SA
OUTPUTNUMBER  1    ! number of output fields 1=mut, 2=1+tvort, 3=2+length-scl

! if TURBMODEL = 1-4 (LES)
CSMAGORINSKY  0.10 ! Model constant, only relevant for TURBMODEL=1
FILTERTYPE    0    ! 0=uniform, 1=non-uniform
DELTATYPE     0    ! 0=cuberoot-formula, 1=squareroot-formula
IFILTERWIDTH  1    ! filterwidth in I-direction/grid-spacing
JFILTERWIDTH  1    ! filterwidth in J-direction/grid-spacing
KFILTERWIDTH  1    ! filterwidth in K-direction/grid-spacing
IHOMOGENDIR   0    ! 0=non-homogeneous, 1=homogeneous I-direction
JHOMOGENDIR   0    ! 0=non-homogeneous, 1=homogeneous J-direction
KHOMOGENDIR   0    ! 0=non-homogeneous, 1=homogeneous K-direction
ENERGYMODEL   1    ! 0=OFF, 1=ACTIVE energy subgrid model
CALCVORTIC    0    ! 0 NO, 1 per fluid-dt, 2 per system-dt

! if TURBMODEL >= 5 (RANS or DES)
WALLDISTMETHOD  0    ! wall distance calc.method: 0 direct, 1 step-wise, 2 PDE
WALLDISTFREQ    0    ! 0 only initial, 1 per-remesh, 2 system-dt, 3 fluid-dt
VISCFUNCTION    0    ! viscous function, SA (fv1): 0= power 3, 1= power 2
CDES            0.65 ! DES lengthscale coefficient
SMOOCF          0.7  ! coeff. of implicit res.smoothing (<0 - no smooth.)
DISCR           1    ! type of space discretization (0=central, 1=upwind-Roe)
K2              0.50 ! artificial dissip. k2 (2nd ord part if central)
1/K4            0.0  ! 1/artificial dissip. k4 (4th ord part if central)
ORDER           1    ! space discr.order: 1=first-order, 2=second-order
#
```

2.1.2 Cautions

- I,J,KHOMOGENDIR. This parameter is of importance for the averaging of the dynamic coefficient if a dynamic LES model is selected. If this input parameter has non-zero value for the l-direction (l is either I, J or K) then that particular direction is

assumed to be homogeneous and the grid in this direction to be uniform. Should there be any change in (i,j,k) orientation between regions, the user should cycle the values of I,J,KHOMOGENDIR and I,J,KFILTERWIDTH accordingly.

- ENERGYMODEL. When this parameter is active (1), the current implementation requires that the turbulence model should have a non-zero value in every region, otherwise an error message will prompt. If user needs to activate turbulence model only in certain regions, then ENERGYMODEL should be turned off. This limitation will be removed in the future (by defining an MPI communicator specific for *rocturb*).

2.1.3 Interdependency of input parameters

The interdependency of input parameters in the .inp file is described in the table

	FLOWTYPE	TURBMODEL	FILTERWIDTH
TURBMODEL	NS steady and unsteady	1-6	
CSMAGORINSKY	NS unsteady	1	
FILTERTYPE	NS unsteady	2-4	=/=(0,0,0)
DELTATYPE	NS unsteady	2-4	=/=(0,0,0)
FILTERWIDTH	NS unsteady	2-4	=/=(0,0,0)
HOMOGENDIR	NS unsteady	3-4	=/=(0,0,0)
ENERGYMODEL	NS unsteady	1-4	=/=(0,0,0)
CALCVORTIC	NS unsteady	1-6	
WALLDISTMETHOD	NS steady and unsteady	5-6	
WALLDISTFREQ	NS unsteady	5-6	
VISCFUNCTION	NS steady and unsteady	5-6	
CDES	NS unsteady	6	
SMOOCF	NS steady and unsteady	5-6	
DISCR	NS steady and unsteady	5-6	
K2	NS steady and unsteady	5-6	
1/K4	NS steady and unsteady	5-6	
ORDER	NS steady and unsteady	5-6	

Table 2.1: Interdependency of input parameters in the .inp file.

2.2 Output Files

The output file for instantaneous turbulent (LES, DES, URANS) and steady state turbulent (RANS) quantities is the .turba file for ASCII format or the .turbb file for binary format. These files may contain 1 up to 3 fields, depending on the parameter OUTPUTNUMBER. Value 1 (default) will give only eddy viscosity field, 2 vorticity field is added, 3 length scale of turbulence model is added (3 is only for RaNS and DES). Eddy viscosity will always

be output since it is needed for exact restart from the use of μ_t in the viscous time step computation. Statistics of turbulence is output in the .stata (ASCII) or .statb (binary). The statistics variables are described in Chapter 3.

Chapter 3

Wall Layer Model and Statistics I/O Files

3.1 Wall Layer Model

There is no output file specific for wlm quantities.

3.1.1 [*CaseName*].bc file

Boundary condition (.bc) file:

```
# BC_WALLMODEL
BLOCK     0  0   ! applies to block ... (0 0 = to all)
PATCH     0  0   ! applies to patch ... (0 0 = to all patches from above range of blocks)
MODEL     2      ! 0=nomodel 1=loglay 2=bndlay 3=external (feed tau_w distribution)
REFPOINT  1      ! reference point (1 to max. wall normal points in the block)
ROUGHNESS 0.0001 ! roughness size [meter]
#
```

3.2 Statistics I/O Files

3.2.1 [*CaseName*].inp file

```
# STATISTICS
DOSTAT     1     ! 1=ON, 0=OFF
RESTART    0     ! restart switch: 1 = continued process, 0 = new process
MIXTNSTAT  11    ! number of mixture statistics with their ID's below
MIXTSTATID 01 02 03 04 06 11 22 33 44 23 66
                 ! 1=rho 2=u 3=v 4=w 5=T 6=p 7=vsound 8=muel 9=tcol 22=uu etc
TURBNSTAT  2     ! number of mixture statistics with their ID's below
TURBSTATID 01 03
                 ! 1=muet 2=tcot 3=cdyn 4:7=t11,t22,t33,t12 8=mmij 9=mlij
PLAGNSTAT  10
PLAGSTATID 01 02 03 04 05 06 07 08 09 44
                 ! 1=diam3 2=diam4 3=numDens 4=u 5=v 6=w 7=mass 8=compAl
                 ! 9=compAl2O3 44=uu
```

#

3.2.2 [*CaseName*].stata/statb file

time, ΔT
MIXTNSTAT MIXTSTATID(1:MIXTNSTAT)
TURBNSTAT TURBSTATID(1:TURBNSTAT)
IREGION ni nj nk ndum
((F_{mixt}(l,ijk), ijk = ijkBeg,ijkEnd), l = 1,NSTAT)
((F_{turb}(l,ijk), ijk = ijkBeg,ijkEnd), l = 1,TURBNSTAT)

Chapter 4

Examples and Test Problems

4.1 Blasius Test Case

4.1.1 blasius.inp file

```
! Input file for blasius case

! mapping of blocks to processors ------------------------------------------

# BLOCKMAP
NBLOCKS   0      ! no. of blocks per processor (0=automatic mapping)
#

! grid/solution format -----------------------------------------------------

# FORMATS
GRID      0      ! 0=Plot3D ASCII, 1=Plot3D binary, 2=HDF
SOLUTION  0      ! 0=ASCII, 1=binary, 2=HDF
#

! viscous/inviscid flow ----------------------------------------------------

# FLOWMODEL
BLOCK  0  0      ! applies to block ... (0 0 = to all)
MODEL     1      ! 0=inviscid (Euler), 1=viscous (Navier-Stokes)
MOVEGRID  0      ! moving grid (0=no, 1=yes)
#

! reference values ----------------------------------------------------------

# REFERENCE
ABSVEL   170.1432 ! absolute velocity [m/s]
PRESS    1.E+5   ! static pressure [Pa]
DENS     1.209   ! density [kg/m^3]
CP       1004.5  ! specific heat coeff. at constant pressure [J/kgK]
GAMMA    1.4     ! ratio of specific heats
LENGTH   0.00529 ! length [m]
RENUM    62500.0 ! Reynolds number (lam. viscosity = dens*absvel*length/renum)
PRLAM    0.72    ! laminar Prandtl number
PRTURB   0.9     ! turbulent Prandtl number
SCNLAM   0.22    ! laminar Schmidt number
SCNTURB  0.9     ! turbulent Schmidt number
#
```

```
! probe ------------------------------------------------------------------------

# PROBE
NUMBER   1
1   1   10   10  ! block, icell, jcell, kcell (1=first physical cell)
2   1   40   10
#

! forces ------------------------------------------------------------------------

# FORCES
TYPE     0       ! 0=no forces calculated, 1=pressure forces, 2=1+viscous forces
#

! multi-physics modules: ---------------------------------------------------------

# TURBULENCE
BLOCK  1  1        ! applies to block ... (0 0 = to all)
TURBMODEL  3       ! 0=laminar, 1=Smag., 2=ScalSim, 3=DynSmag., 4=DynMix, etc.
CSMAGORINSKY  0.05
FILTERTYPE    0
DELTATYPE     0
IFILTERWIDTH  1
JFILTERWIDTH  1
KFILTERWIDTH  1
IHOMOGENDIR   0
JHOMOGENDIR   0
KHOMOGENDIR   0
ENERGYMODEL   1
#

# TURBULENCE
BLOCK  2  2        ! applies to block ... (0 0 = to all)
TURBMODEL  3       ! 0=laminar, 1=Smag., 2=ScalSim, 3=DynSmag., 4=DynMix, etc.
CSMAGORINSKY  0.05
FILTERTYPE    0
DELTATYPE     0
IFILTERWIDTH  1
JFILTERWIDTH  1
KFILTERWIDTH  1
IHOMOGENDIR   0
JHOMOGENDIR   0
KHOMOGENDIR   0
ENERGYMODEL   1
#

# SPECIES
BLOCK  0  0      ! applies to block ... (0 0 = to all)
MODEL  0         ! 0=perfect gas, 1=...
#

# CONPART
BLOCK  0  0      ! applies to block ... (0 0 = to all)
USED   0         ! 0=module not used
#

# DISPART
BLOCK  0  0      ! applies to block ... (0 0 = to all)
USED   0         ! 0=module not used
#

# RADIATION
BLOCK  0  0      ! applies to block ... (0 0 = to all)
USED   0         ! 0=module not used
```

```
#

! time-stepping control ---------------------------------------------------

# TIMESTEP
FLOWTYPE   1      ! 0=steady flow, 1=unsteady flow

! if FLOWTYPE=0
TIMESTEP   5.E-8  ! max. physical time step [s]
STARTTIME  2.E-7  ! current time
MAXTIME    4.E-7  ! max. time simulated [s]
WRITIME    1.E-5  ! time offset [s] to store solution
PRNTIME    5.E-8  ! time offset [s] to print convergence

! if FLOWTYPE=0
STARTITER  0      ! current iteration
MAXITER    20     ! max. number of iterations
RESTOL     1.E-5  ! max. density residual to stop iterations
WRIITER    1000   ! offset between iterations to store solution
PRNITER    2      ! offset between iterations to print convergence
#

! time averaged statistics for unsteady flow ----------------------------------

# STATISTICS
DOSTAT     0     ! 1=ON, 0=OFF
RESTART    1     ! restart switch: 1 = continued process, 0 = new process
MIXTNSTAT  6     ! number of MIXT statistics variables with their ID's below
MIXTSTATID  01 02 03 04 05 33 34
                 ! 1=rho,2=u,3=v,4=w,5=T,6=p,7=vsound,8=muel,9=tcol,22=uu,etc
TURBNSTAT  2     ! number of TURB statistics variables with their ID's below
TURBSTATID  01 03
                 ! 1=muet, 2=tcot, 3=cdyn
#

! numerics ------------------------------------------------------------------

# MULTIGRID
START    1       ! at which grid level to start (>0; 1=finest grid)
CYCLE    0       ! 0=no MG, 1=V-cycle, 2=W-cycle
REFINE   99999   ! no. of iterations before switching to next finer grid
#

# NUMERICS
BLOCK    0  0    ! applies to block ... (0 0 = to all)
CFL      7.0     ! CFL number
SMOOCF   0.7     ! coefficient of implicit residual smoothing (<0 - no smooth.)
DISCR    0       ! type of space discretization (0=central, 1=Roe, 2=MAPS)
K2       0.0     ! dissipation coefficient k2 (if discr=0)
1/K4     128.    ! dissipation coefficient 1/k4 (if discr=0)
ORDER    2       ! 1=first-order, 2=second-order, 4=fourth-order
LIMFAC   5.0     ! limiter coefficient (if discr=1)
ENTROPY  0.05    ! entropy correction coefficient (if discr=1)
#
```

4.1.2 blasius.top file for single processor run

```
# topology file for Blasius flow - 1 block
#
 1      ! total no. of blocks
 1  1   ! block, no. of grid levels
 6  2   25  64           ! no. of patches, icells, jcells, kcells
```

```
100  1   1  25   1  64    0   0   0   0   0   0   0
100  2   1  25   1  64    0   0   0   0   0   0   0
 10  3   1  64   1   2    0   0   0   0   0   0   0
 20  4   1  64   1   2    0   0   0   0   0   0   0
100  5   1   2   1  25    0   0   0   0   0   0   0
 60  6   1   2   1  25    0   0   0   0   0   0   0
```

4.1.3 blasius.top file for multi processors run

```
# topology file for Blasius flow - 2 blocks
#
 2      ! total no. of blocks
 1  1   ! block, no. of grid levels
 6  2  25  64            ! no. of patches, icells, jcells, kcells
100  1   1  25    1  64    0   0   0   0   0   0   0 ! type, lb, l1beg, l1end, l2beg, l2end
100  2   1  25    1  64    0   0   0   0   0   0   0 ! <0 => coord. aligned
 10  3   1  64    1   2    0   0   0   0   0   0   0
 30  4  -1 -64    1   2    2   3  -1 -64   1   2   0
 60  5   1   2    1  25    0   0   0   0   0   0   0
100  6   1   2    1  25    0   0   0   0   0   0   0
 2  1   ! block, no. of grid levels
 6  2  100  64            ! no. of patches, icells, jcells, kcells
100  1   1  100   1  64    0   0   0   0   0   0   0
100  2   1  100   1  64    0   0   0   0   0   0   0
 30  3  -1  -64   1   2    1   4  -1 -64   1   2   0
 20  4   1   64   1   2    0   0   0   0   0   0   0
 70  5   1    2   1 100    0   0   0   0   0   0   0
100  6   1    2   1 100    0   0   0   0   0   0   0
```

4.1.4 Comparison result of Blasius case

Figure 5.1 shows comparison of compressible Blasius solution at Mach 0.5 between Rocflo (black) and analytical solution (blue). The two solution shows virtually perfect collapse.

Chapter 5

Rocturb Verification and Validation

5.1 Analytical Field

The expression of a turbulence model applied on an analytical flow can be exactly derived. Therefore an analytical flow is imposed as initial condition to check whether the turbulence model gives the correct result. This check is currently done for the Smagorinsky model (see Rocturb Developer's guide for model description)

$$\mu_t = \rho C_s^2 \Delta^2 |S|. \tag{5.1}$$

We consider an analytical flow which vary only in the x_1 direction first

$$u_1 = \sin 2x_1 \tag{5.2}$$
$$u_2 = \cos 2x_1 \tag{5.3}$$
$$u_3 = 0. \tag{5.4}$$

It can easily be derived that the expression for the strain rate tensor magnitude is

$$|S| = 2(1 + \frac{1}{3}\cos^2 2x_1)^{\frac{1}{2}}. \tag{5.5}$$

Defining the maximum error as

$$\mathrm{err}_{max} = \max\Big(\frac{|\mu_{t-analytic} - \mu_{t-R4.0}|}{|\mu_{t-analytic}|}\Big) \tag{5.6}$$

the maximum (discretization) error introduced by Rocflo-Rocturb as function of grid refinement in the x_1 direction with nj=32 and nk=2 is shown on the left hand side of table 5.1. Next we also check on an analytical flow which vary only in the x_2 direction first

$$u_1 = \sin 2x_2 \tag{5.7}$$
$$u_2 = \cos 2x_2 \tag{5.8}$$
$$u_3 = 0. \tag{5.9}$$

ni	err_{max}		nj	err_{max}
32	1.6056069 E-3		32	6.4131489 E-3
64	4.0154685 E-3		64	1.6056069 E-3
128	1.0039578 E-4		128	4.0154685 E-3
256	2.5099513 E-5		256	1.0039578 E-4
512	6.2749139 E-6		512	2.5099513 E-5

Table 5.1: Maximum errors for the x_1 (left) and x_2 (right) varying flow field

The expression for the strain rate tensor magnitude is given by

$$|S| = 2(1 + \frac{1}{3}\sin^2 2x_2)^{\frac{1}{2}}. \tag{5.10}$$

The maximum (discretization) error introduced by Rocflo-Rocturb as function of grid refinement in the x_2 with ni=32 and nk=2 is shown on the right hand side of table 5.1. The test shows that the convergence rate with the grid refinement is of factor 4 which implies the second order accuracy. Note that the x_2 varying function introduced higher errors. This is because the test is done on μ_t defined at i-faces and the x_2 varying function involves an additional interpolation procedure. This in fact also shows that the interpolation is second order accurate.

5.2 Compressible Periodic Rocket (CPR)

To check the implementation of the CPR modules we perform validations in laminar and turbulent regimes of the flow. The laminar validation consists of mean flow comparison and linear stability analysis. The turbulent validation involves comparison of mean flow as well as rms of fluctuations. For the reference data we use corresponding results from other tested codes and DNS data for turbulence.

5.2.1 Laminar

In this section the CPR test case in the laminar regime is presented. The case corresponds to the state of the flow near the head end of the rocket. For the mean flow validation the laminar flow simulation is initiated using Cullick's solution for the inviscid rocket flow, which can be thought as a plane channel flow but with finite wall normal velocities instead of no slip walls (see RocCPR Developer's guide and paper of Prem *et al.* 2000). This solution forms a reasonable initial condition for the present compressible flow case. Specifically the following reference Reynolds number, density, length, velocity and temperature in SI units are employed:

$$Re = 5000,\ \rho_r = 4.2294\ \text{kg/m}^3,\ V_r = 323.215\ \text{m/s},\ \delta = 1.0\ \text{m and}\ T_r = 260\ \text{K}.$$

The injection ratio is $\epsilon = 0.1$. The grid is uniform with size ni=nj=65, nk=2 in the streamwise, wall normal and spanwise direction. The computational domain is a box with dimension $L_x = \pi,\ L_y = 2.0$ and $L_z = 0.05$ in the corresponding direction.

The mean flow at quasi steady state is represented in fig.5.2-fig.5.6 for density, velocities, temperature and pressure, respectively. It is called quasi steady state as the flow is absolutely unstable and hence the linear regime is not durable in a simulation using finite volume/difference method due to the incurrence of spurious modes triggered by truncation errors. Non linear interactions between spurious modes can be suppressed by increasing the numerical dissipation, but it is not done in this case. The figures show how the solution has evolved from the initial condition. They also show that the mean flow virtually collapse with the reference data, which is obtained from a different code based on spectral method where the solution is truly steady state.

We next perform a two dimensional linear stability analysis to check if small perturbations behave correctly in this laminar regime. As initial condition we imposed the above steady state mean flow, which also forms the base flow, added with linear eigen function perturbations,

$$\begin{aligned} \rho &= \overline{\rho} + \widetilde{\rho}, & p &= \overline{p} + \widetilde{p}, & T &= \overline{T} + \widetilde{T}, \\ u_1 &= \overline{U}_1 + \widetilde{u}_1, & u_2 &= \overline{U}_2 + \widetilde{u}_2, \end{aligned}$$

where the bars denote the base flow and the tildes the perturbations. The perturbation is assumed represented by a harmonic wave of the form

$$(\widetilde{\rho}, \widetilde{u_1}, \widetilde{u_2}, \widetilde{p}, \widetilde{T}) = [\widehat{\rho}(x_2), \widehat{u_1}(x_2), \widehat{u_2}(x_2), \widehat{p}(x_2), \widehat{T}(x_2)] e^{i(\alpha x_1 - \omega t)}. \tag{5.11}$$

The spanwise velocity component is set to zero as the problem is restricted to two dimensional. The hats denote the perturbation eigen function, α the streamwise wave number and ω, which is complex, the circular frequency for the real part and the growth rate for the imaginar part. We set the wave number $\alpha = 2$, which implies that one wave length fits precisely within the streamwise extent $L_x = \pi$. The contours of the eigen function perturbations are shown in fig.5.7 and fig.5.8. The linear stability analysis results in the following dimensional values of ω

$$\omega = \omega_r + \omega_i = 60.0716 - i1.4242,$$

which serves as the reference value. The corresponding estimations given by ROCFLO_4.0 are

$$\omega = \omega_r + \omega_i = 60.2518 - i1.0713,$$

for grid 65x65x2 and

$$\omega = \omega_r + \omega_i = 60.0304 - i1.3582,$$

for grid 65x129x2. Grid refinement in the wall normal direction clearly improves the estimation. It should be noted, however, that the fourth order artificial dissipation should be

set to a sufficient level (about 0.016) in order for this particular mode to have a reasonable temporal extent. Lower artificial dissipation results in the incurrence of subharmonic waves with much higher frequency and growth rate.

5.2.2 Turbulent

In this section CPR test cases in the turbulent regime are presented. Two turbulent simulations are carried out. First without any turbulence model in order to compare with results previously obtained by the old ROCFLO_3.2 and second, using Smagorinsky LES model to investigate the effect of the model qualitatively. Other than the turbulence model option, the physical parameters are the same for the two cases. The simulations are carried out at the injection ratio $\epsilon = 0.025$ and Reynold number 2000, which corresponds to the state of flow further downstream from the rocket head end. The reference quantities are given by

$$\rho_r = 3.28 \text{ kg/m}^3,\ V_r = 158.36 \text{ m/s},\ \delta = 1.0 \text{ m and } T_r = 260 \text{ K}.$$

The size of the flow domain is $L_x = 4\pi,\ L_y = 2.0$ and $L_z = 2\pi$ meshed by uniform grid 121x65x64 in the corresponding direction.

The mean flow components are presented in fig.5.9-fig.5.13 for the density, velocities, temperature and pressure, respectively. The figures show comparison between Rocflo no-model, Rocflo with Smagorinsky model and the old ROCFLO_3.2 no-model. The last employes the same physical and numerical parameters as the present simulations and is considered as the reference. The difference between current Rocflo and the older version is only visible in the density and pressure, and is virtually negligible. This is encouraged by the agreement in the rms values of the fluctuations as shown further below. The relative deviation in the mean density and mean pressure is 0.5% and 0.7%, respectively. Although the numerical method used in current Rocflo and ROCFLO_3.2 is basically the same, ROCFLO_3.2 is a single precision code whereas current Rocflo is double precision. The shown results of ROCFLO_3.2 is initiated with an initial flow that is different from the one used in current Rocflo. The no-model solution is estimately close to quasi DNS by checking the model stress of the simulation with the Smagorinsky model. The model stress is small compared to the resolved stress. The effect of the Smagorinsky model is that this model tends to laminarize the flow. This is considered as qualitatively correct as the Smagorinsky model is well known of its dissipative character.

The comparison of the fluctuations is presented in fig.5.14-fig.5.18 which show virtually the same rms values between the two codes. The rms values of the simulation with Smagorinsky model are generally not much smaller than the corresponding no-model values (note that the vertical axis is not always originated at zero) and the difference occurs mostly closer to the walls than the core region. This indicates that the model contribution is relatively small and only active near the walls where the strain rate is high due to the vanishing streamwise velocity.

5.3 Turbulent Channel Flow at Various Reynolds Numbers

This section is partly taken from the paper by Wasistho *et al.* [15]. We performed verification of log-law based wall layer model and DES in a plane channel flow. As can be seen in the plot of logarithmic profiles in Figure 5.19, five testcases are considered, namely full LES at $Re_\tau = 180$ (A), LES+WLM at $Re_\tau = 1000$ (B) and $Re_\tau = 3000$ (C), DES at $Re_\tau = 2000$ (D), and RaNS-SA at $Re_\tau = 3000$ (E). The dimension for all cases is $2\pi h \times 2h \times \pi h$, in the streamwise, wall normal, and spanwise direction, respectively, except for case A which employs $2\pi h \times 2h \times 4/3\pi h$, with $h = 0.01m$. The grid size for case A is $64 \times 128 \times 64$ while for the high Reynolds number cases is $64 \times 64 \times 32$. The bulk velocity is equivalent to a bulk Mach number of 0.5, implying low compressibility effect. The low Reynolds number LES, case A, captures the universal log law accurately. LES+WLM at $Re_\tau = 1000$ and 3000, case B and C, are in reasonable agreement with the theory. We observe that the slope of case C deviates slightly and this trend continues at Reynolds numbers above $Re_\tau = 3000$ indicating the need to increase the grid resolution. Case D, which is DES at $Re_\tau = 2000$, produces an adjustment in the log profile, typical for DES of channel flow [9]. This manifests in a higher intercept in the LES region which implies underprediction of the skin friction. DES can, however, be applied at much higher Reynolds numbers without a severe penalty in grid size. Case E, RaNS at $Re_\tau = 3000$, aligns with the theory, as expected.

We computed an additional case not included in Figure 5.19, namely coarse grid LES without WLM at $Re_\tau = 1000$, for convenience called case F. The rms values of streamwise and wall normal velocity fluctuations, normalized by the friction velocity, are shown in Figure 5.20 and 5.21, respectively. In these figures B and F are compared with the DNS data of del Alamo *et al.* [2] at $Re_\tau = 950$. Figure 5.20 shows that the level of the near wall peaks in u fluctuations in case B are comparable to those of the DNS data, thanks to the wall layer model. The fluctuations level away from the wall is however underestimated by the simulation using WLM. Case F on the other hand overestimates the rms values by a factor of nearly two near the wall, although less severe in the core region. This overestimation is due to the underprediction of the skin friction or equivalently the friction velocity which is used for the normalization of the rms quantities. A similar result is shown for the rms of wall normal fluctuations in Figure 5.21. The LES using WLM is in close agreement with DNS. The near wall peaks are however located farther from the walls compared to DNS. Case F, on the other hand, significantly overestimates the rms value throughout the channel cross section.

Figure 5.22 and 5.23 show the stress components of DES at $Re_\tau = 180$, which is virtually the same as LES at the same Reynolds number (case A), and DES at $Re_\tau = 3000$ (case D), respectively. Comparing these figures, the model contribution of DES becomes more dominant with the increasing Reynolds number. The opposite holds for the viscous contribution, while the resolved components are comparable between the two cases. We obtain qualitatively the same DES result as in the incompressible counterpart reported by Nikitin *et al.* [9]. It was found that using second order central discretization for the turbulence model

equation yields a better result than first order upwind. In contrast to the incompressible DES, where a semi implicit method is used, we employ a fully explicit RK4 scheme for both NS and SA equations in this study. A multi stage explicit scheme is used for the steady state calculation of fully RaNS case, such as case E. Further investigation is needed on the time discretization of DES, among others by considering a dual time stepping method.

5.4 Papers on Rocturb Verification and Validation

Other Rocturb verification and validation cases can further be found in journal papers [14], [15], and [16].

Bibliography

[1] Bardina, J., Ferziger, J.H., and Reynolds, W.C. (1984). Improved turbulence models based on LES of homogeneous incompressible turbulent flows. Department of Mechanical Engineering. *Report No. TF-19*, Stanford.

[2] del Alamo, J.C., Jimenez, J., Zandonade, P., and Moser, R.D. (2004). Scaling the energy spectra of turbulent channels. *J. Fluid Mech.*, **500**, 2004, 135-144.

[3] Durbin, P.A. (1991). Near wall turbulence clossure modeling without damping functions. *Theoretical Comp. Fluid Dynamics*, **3**, No. 1, 1-13.

[4] Germano, M., Pilmelli, U., Moin, P., and Cabot, W.H. (1991). A dynamic subgrid scale eddy viscosity model. *Phys. Fluids A*, **3**, 1760-1765.

[5] Germano, M. (1992). Turbulence: the filtering approach. *J. Fluid Mech.*, **238**, 325-336.

[6] Hoffman, G., and Benocci, C. (1994). Approximate wall boundary conditions for LES", 5th Advances in Turbulence, ed. R. Benzi, pp.222-28. Dordrecht: Kluwer.

[7] Jones, W.P., and Launder, B.E. (1972). The prediction of laminarization with a two equation model of turbulence. *International J. of Heat and Mass Transfer*, **15**, 301-314.

[8] Launder, B.E., and Sharma, B.I. (1974). Application of the energy dissipation model of turbulence to the calculation of flow near a spinning disc. *Letters in Heat and Mass Transfer*, **1**, No. 2, 131-138.

[9] Nikitin, N.V., Nicoud, F., Wasistho, B., Squires, K.D., and Spalart, P.R. (2000). An approach to wall modeling in large eddy simulations. *Phys. Fluids*, **12**, No. 7, 1629-1632.

[10] Smagorinsky, J. (1963). General circulation experiments with the primitive equations. *Mon. Weather Rev.*, **91**, 99-164.

[11] Venugopal, P., Najjar, F.M., and Moser, R.D. (2000). DNS and LES computations of model solid rocket motors. *AIAA 2000-3571,* 36^{th} *AIAA/ASME/SAE/ASEE Joint Propulsion Conference and Exhibit*, Huntsville, AL, July 16-19.

[12] Spalart, P.R., and Allmaras, S.R. (1994). A oner equation turbulence model for aerodynamic flows'. *La Recherche Aerospatiale*, No. 1, 5-21.

[13] Vreman, B., Geurts, B., and Kuerten, H. (1994). On the formulation of dynamic mixed subgrid scale model.*Phys. Fluids*, **6**, 4057-4059.

[14] Wasistho, B., Balachandar, S., and Moser, R.D. (2004). Compressible Wall-Injection Flows in Laminar, Transitional, and Turbulent Regimes: Numerical Prediction. *AIAA Journal of Spacecraft and Rocket*, to appear, **41**, No. 6, 915-924.

[15] Wasistho, B., and Moser, R.D. (2005). Simulation strategy of turbulent internal flow in solid rocket motor. *J. Propulsion Power*, **21**, No. 2.

[16] Wasistho, B., Najjar, F., Haselbacher, A., Balachandar, S. and Moser, R.D. Effect of Turbulence and Particle Combustion on Solid Rocket Motor Instabilities, AIAA 2005-4345, Joint Propulsion Conference 2005, Tucson, AZ.

[17] Werner, H., and Wengle, H. (1991). Large eddy simulation of turbulent flow over and around a cube in a plate channel. *Proceedings of the* 8^{th} *Symposium on Turbulent Shear Flows*, Technical Univ., Munich, Germany, 19.4.1-19.4.6.

[18] Zang, Y., Street, R.L., and Koseff, J.R. (1993). A dynamic mixed subgrid scale model and its application to turbulent recirculating flows. *Phys. Fluids A*, **5**, 3186-3196.

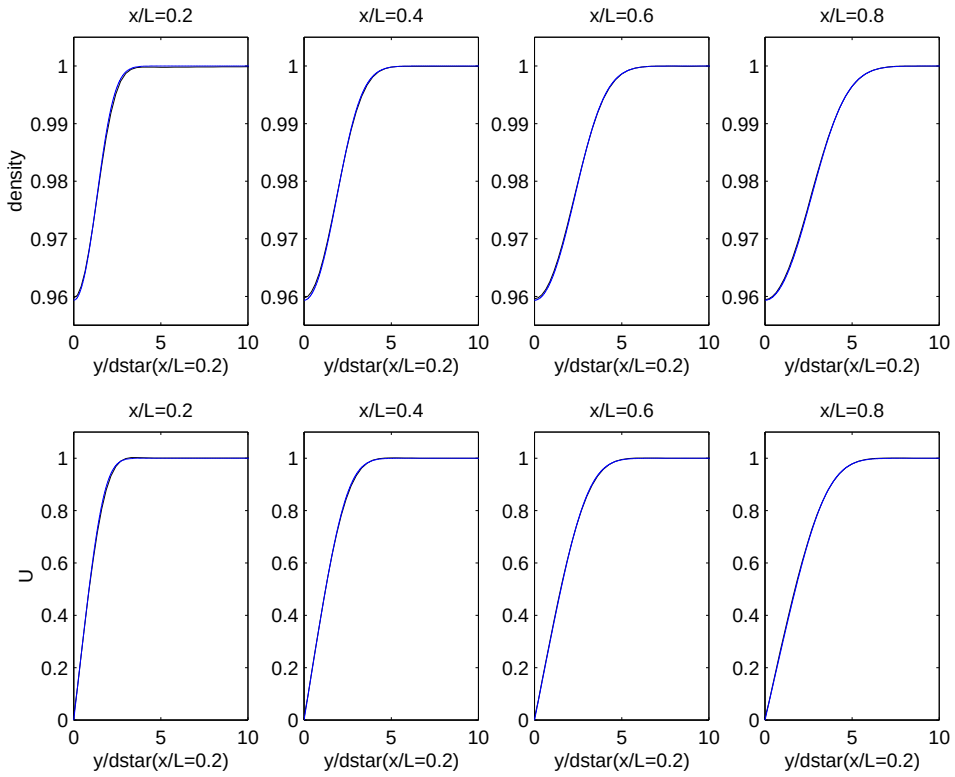

Figure 5.1: Comparison of compressible Blasius solution at Mach 0.5 between Rocflo (black) and analytical solution (blue) for density (upper figures) and streamwise velocity (lower figures).

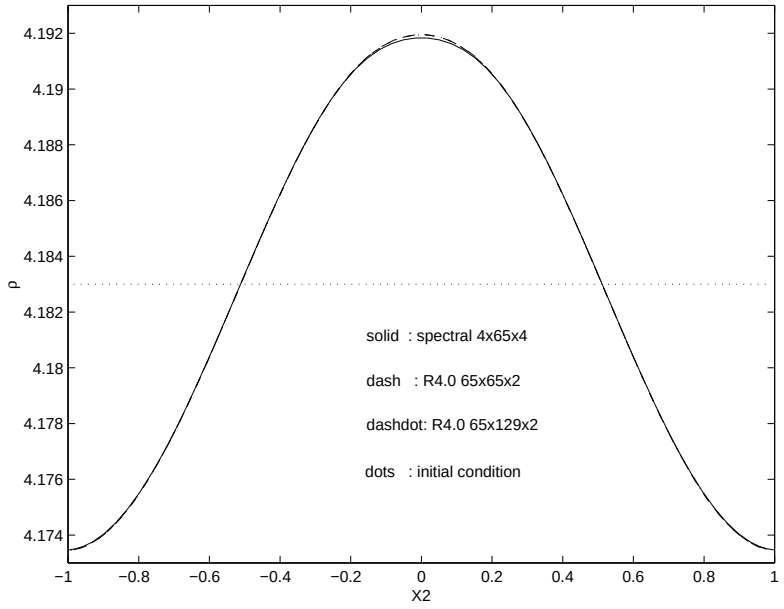

Figure 5.2: Mean density of laminar CPR: spectral 4x65x4 (solid), R4.0 65x65x2 (dash), R4.0 65x129x2 (dashdot), initial condition (dots).

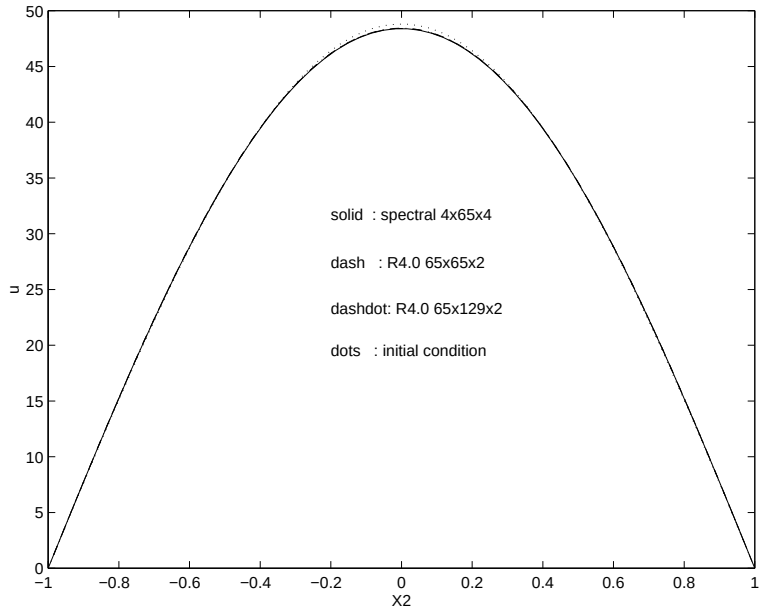

Figure 5.3: Mean streamwise velocity of laminar CPR: spectral 4x65x4 (solid), R4.0 65x65x2 (dash), R4.0 65x129x2 (dashdot), initial condition (dots).

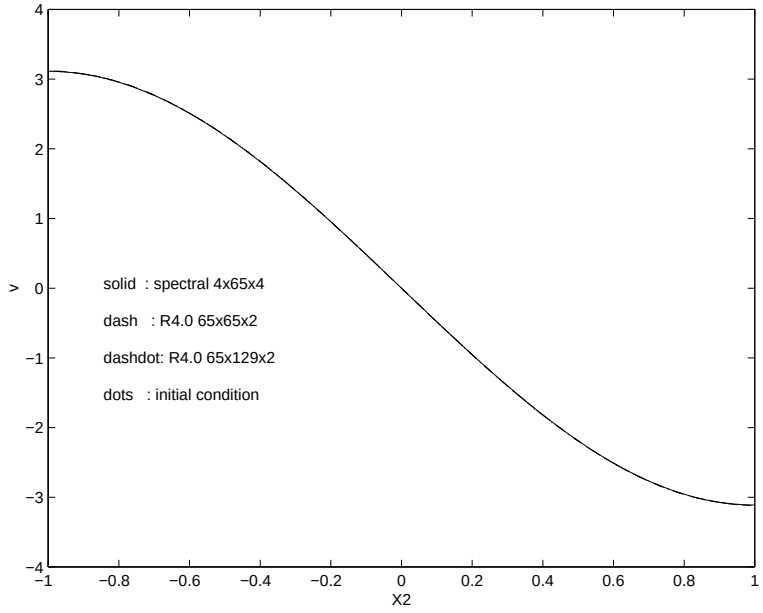

Figure 5.4: Mean wall normal velocity of laminar CPR: spectral 4x65x4 (solid), R4.0 65x65x2 (dash), R4.0 65x129x2 (dashdot), initial condition (dots).

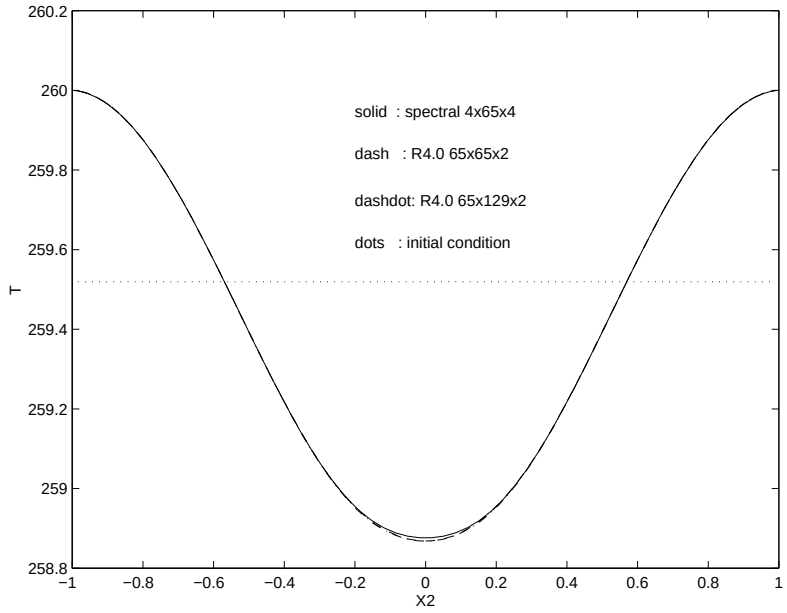

Figure 5.5: Mean temperature of laminar CPR: spectral 4x65x4 (solid), R4.0 65x65x2 (dash), R4.0 65x129x2 (dashdot), initial condition (dots).

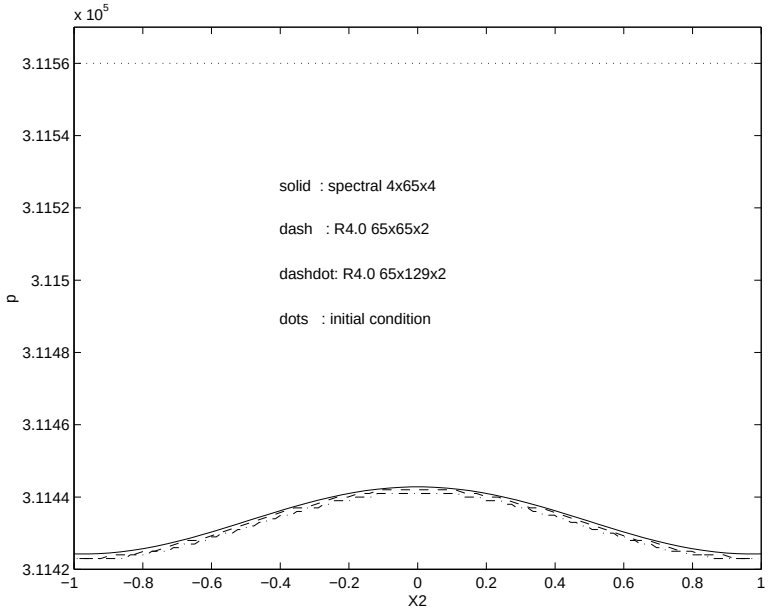

Figure 5.6: Mean pressure of laminar CPR: spectral 4x65x4 (solid), R4.0 65x65x2 (dash), R4.0 65x129x2 (dashdot), initial condition (dots).

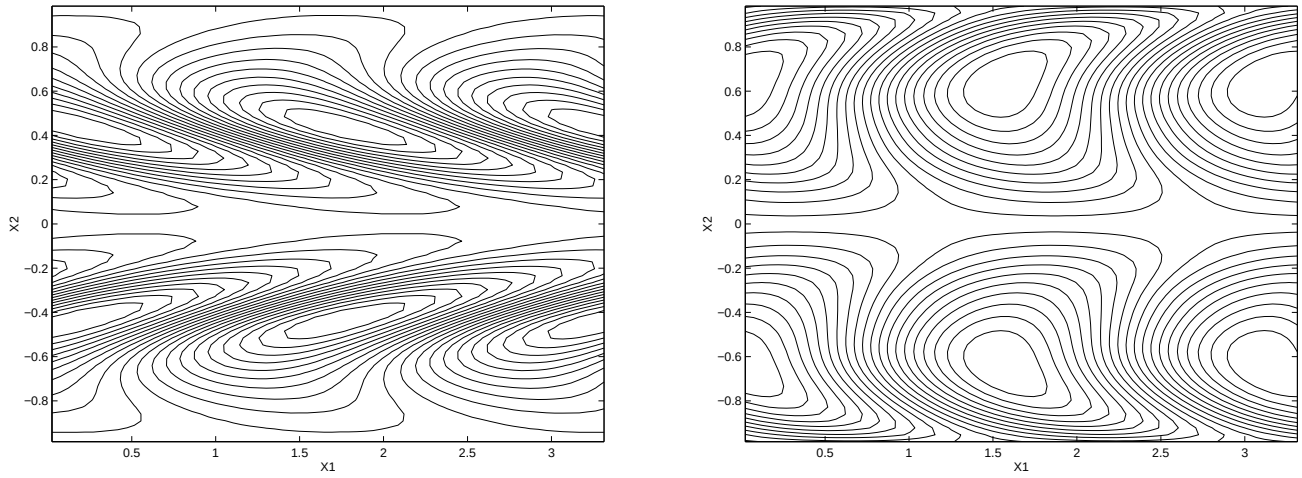

Figure 5.7: Contours of eigen function perturbations: density component (left) and streamwise velocity component (right).

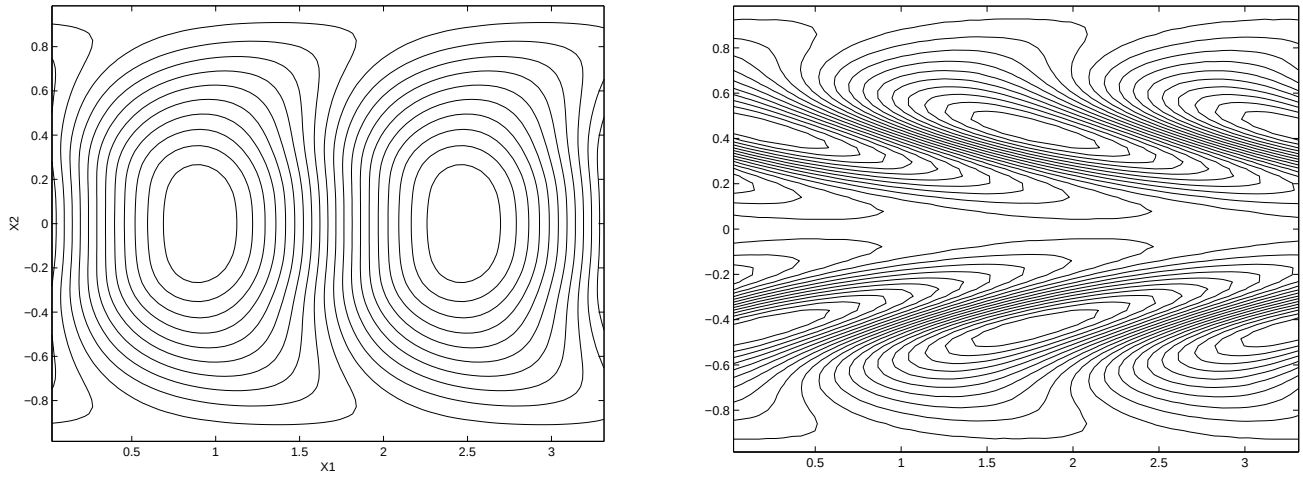

Figure 5.8: Contours of eigen function perturbations: wall normal velocity component (left) and temperature component (right).

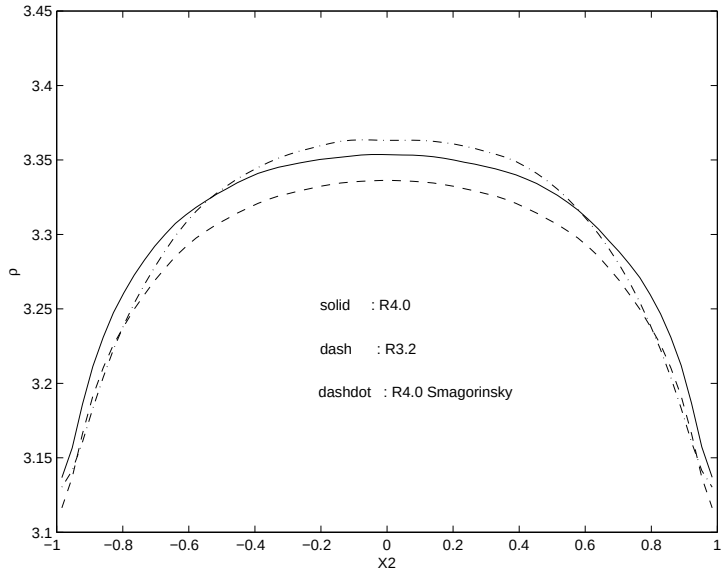

Figure 5.9: Mean density of turbulent CPR: R3.2 no-model (dash), R4.0 no-model (solid), R4.0 Smagorinsky (dashdot).

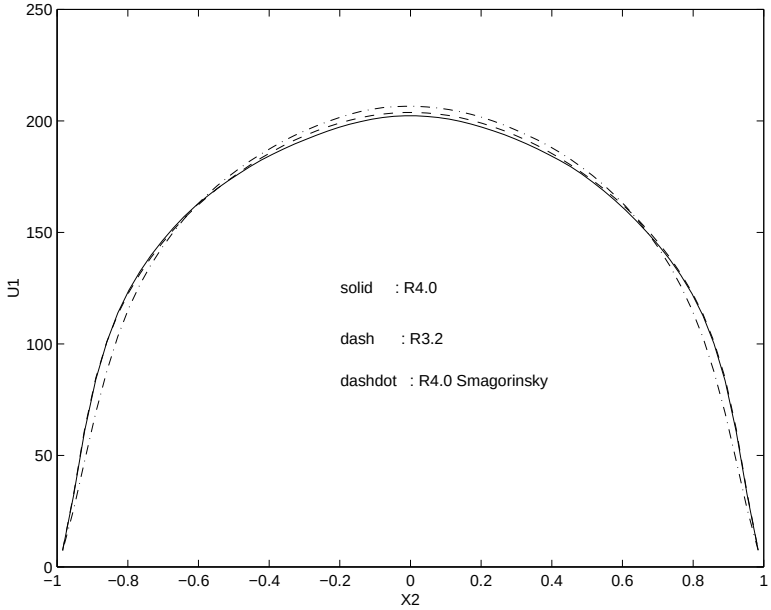

Figure 5.10: Mean streamwise velocity of turbulent CPR: R3.2 no-model (dash), R4.0 no-model (solid), R4.0 Smagorinsky (dashdot)

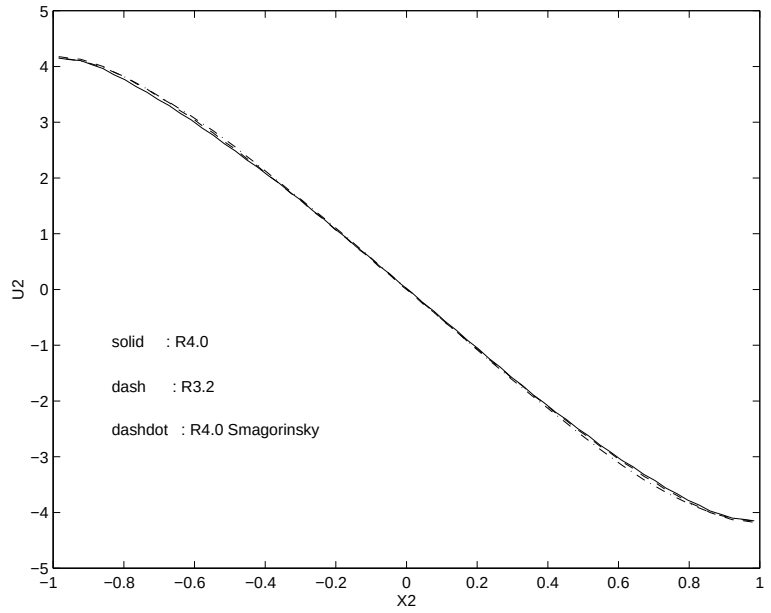

Figure 5.11: Mean wall normal velocity of turbulent CPR: R3.2 no-model (dash), R4.0 no-model (solid), R4.0 Smagorinsky (dashdot).

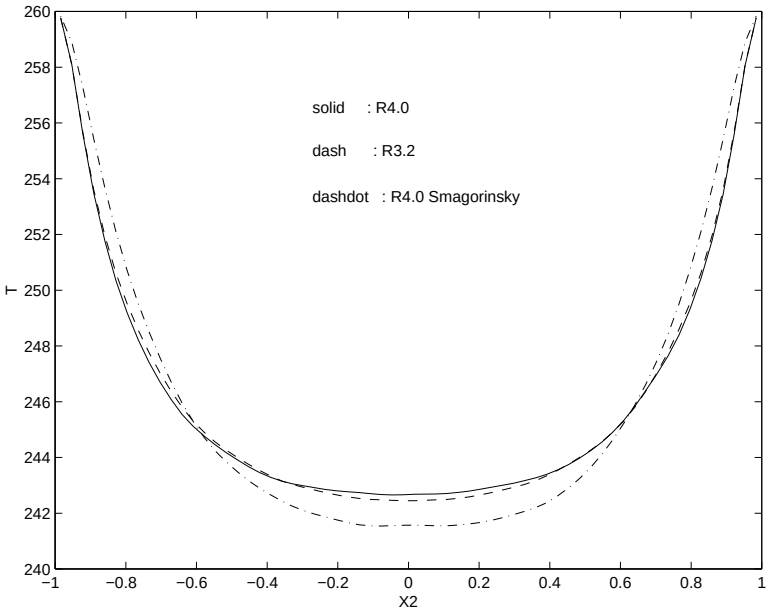

Figure 5.12: Mean temperature of turbulent CPR: R3.2 no-model (dash), R4.0 no-model (solid), R4.0 Smagorinsky (dashdot)

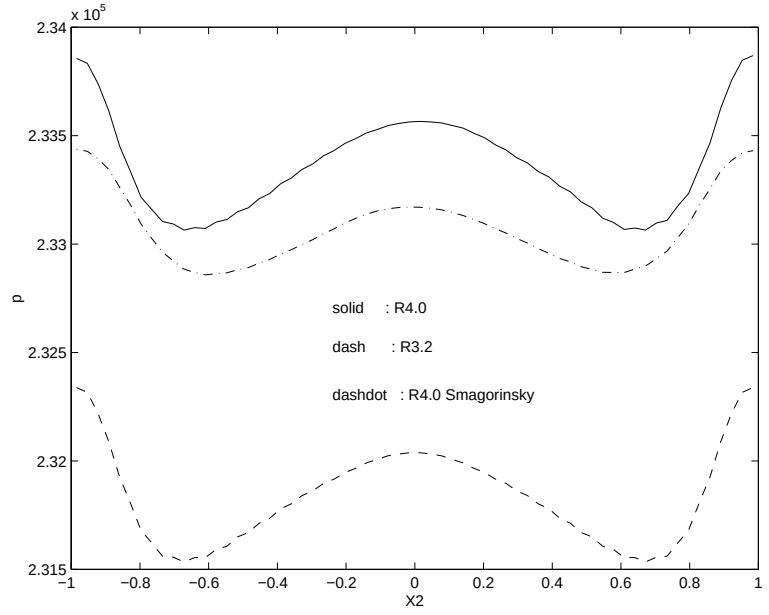

Figure 5.13: Mean pressure of turbulent CPR: R3.2 no-model (dash), R4.0 no-model (solid), R4.0 Smagorinsky (dashdot).

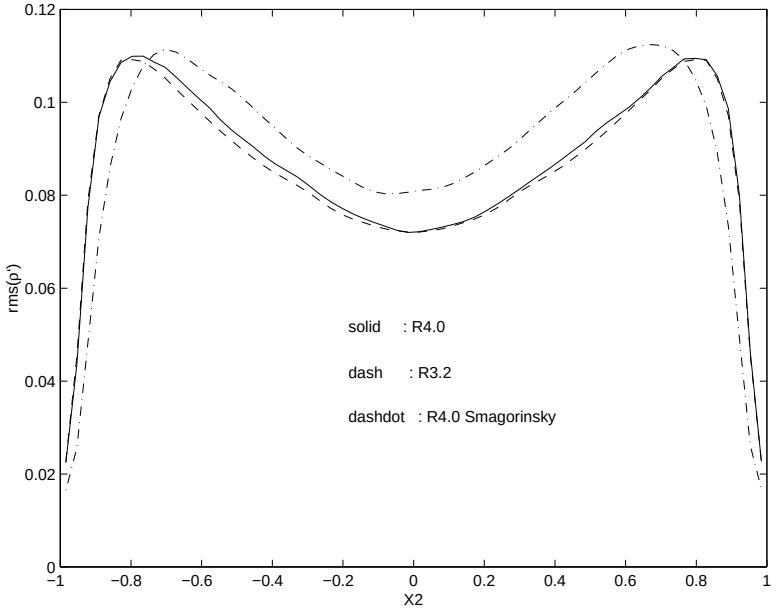

Figure 5.14: R.m.s of density fluctuations in turbulent CPR: R3.2 no-model (dash), Rocflo no-model (solid), Rocflo Smagorinsky (dashdot).

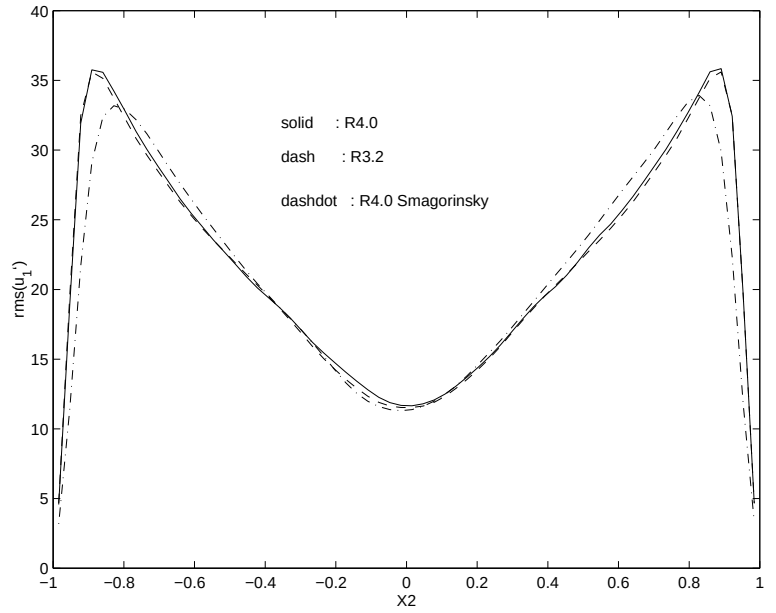

Figure 5.15: R.m.s of streamwise velocity fluctuations in turbulent CPR: R3.2 no-model (dash), Rocflo no-model (solid), Rocflo Smagorinsky (dashdot).

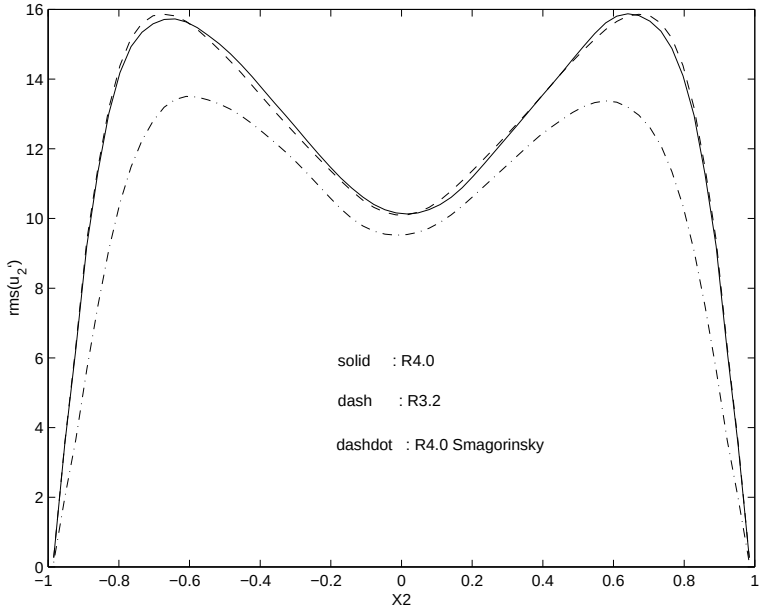

Figure 5.16: R.m.s of wall normal velocity fluctuations in turbulent CPR: R3.2 no-model (dash), Rocflo no-model (solid), Rocflo Smagorinsky (dashdot).

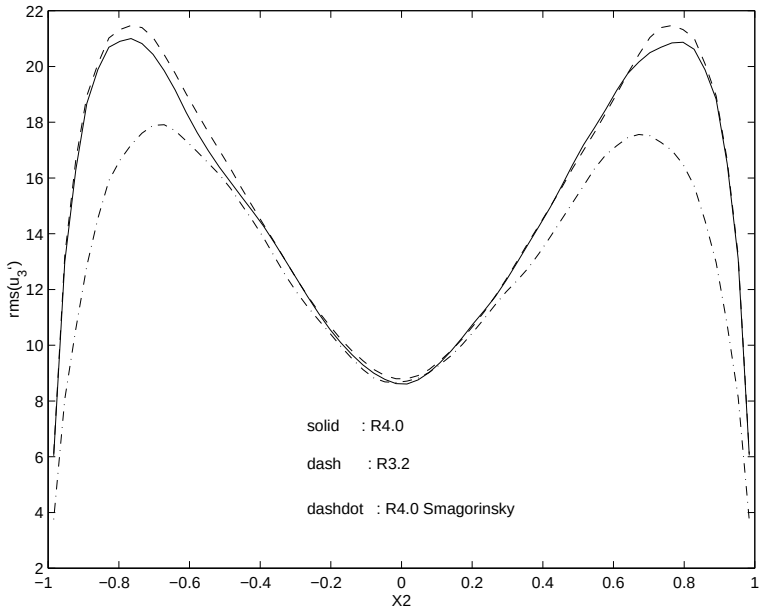

Figure 5.17: R.m.s of spanwise velocity fluctuations in turbulent CPR: R3.2 no-model (dash), Rocflo no-model (solid), Rocflo Smagorinsky (dashdot).

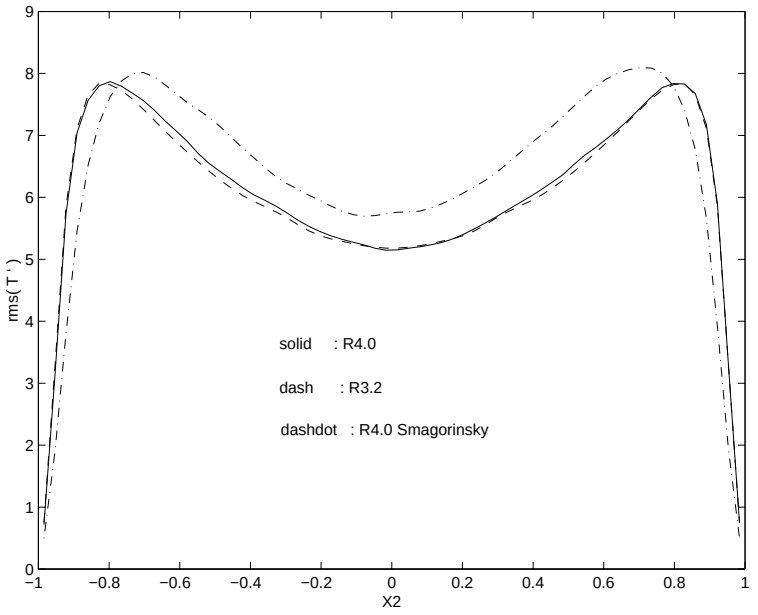

Figure 5.18: R.m.s of temperature fluctuations in turbulent CPR: R3.2 no-model (dash), Rocflo no-model (solid), Rocflo Smagorinsky (dashdot).

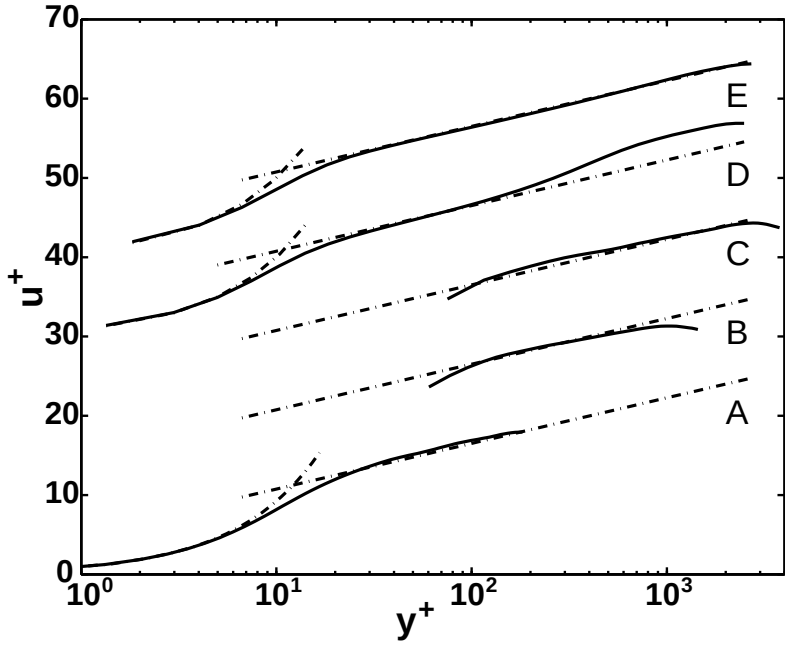

Figure 5.19: Channel flow logarithmic profiles of LES $Re_\tau = 180$ (A), LES+WLM $Re_\tau = 1000$ (B), LES+WLM $Re_\tau = 3000$ (C), DES $Re_\tau = 2000$ (D) and RaNS-SA $Re_\tau = 3000$ (E)

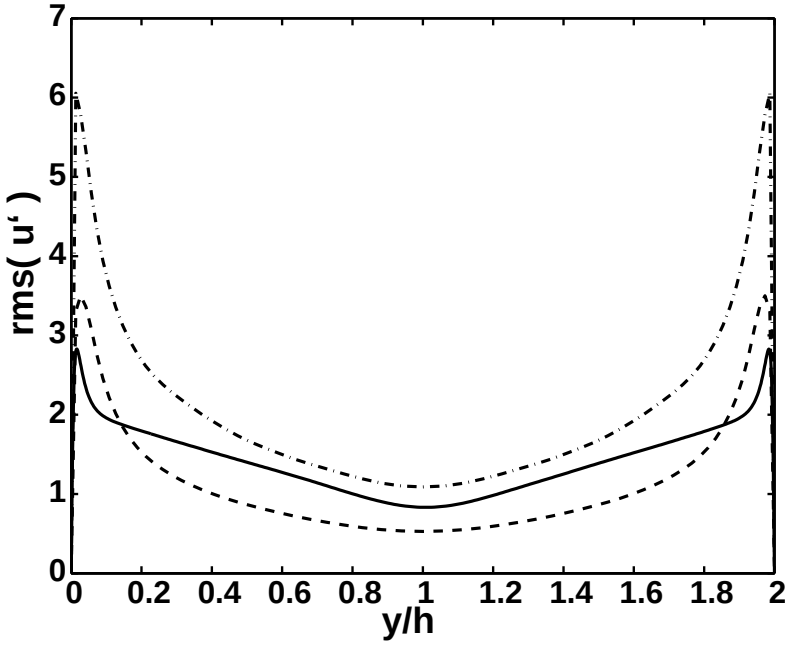

Figure 5.20: Rms of streamwise velocity fluctuations of DNS $Re_\tau = 950$ (solid), LES+WLM $Re_\tau = 1000$ (dash), LES $Re_\tau = 1000$ (without wall model) (dashdot)

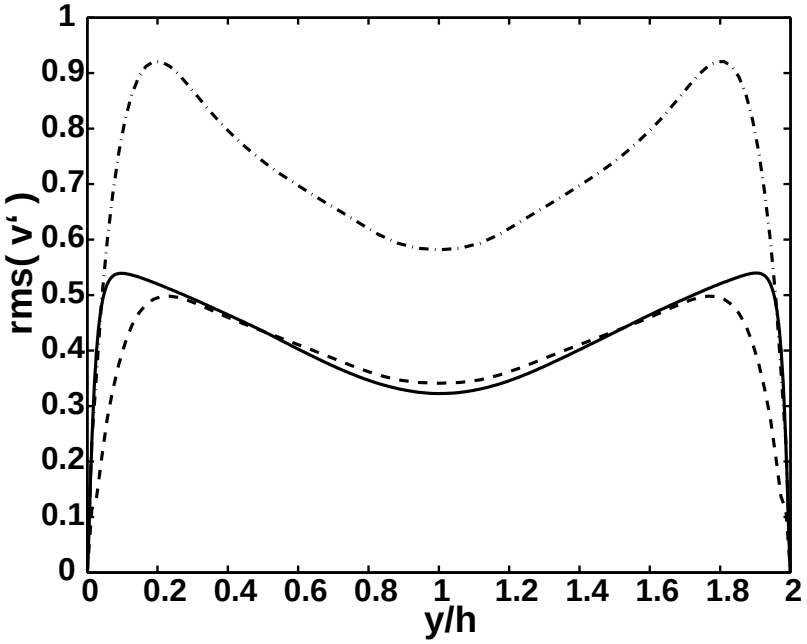

Figure 5.21: The same comparison as previous figure for rms of wall normal velocity fluctuations.

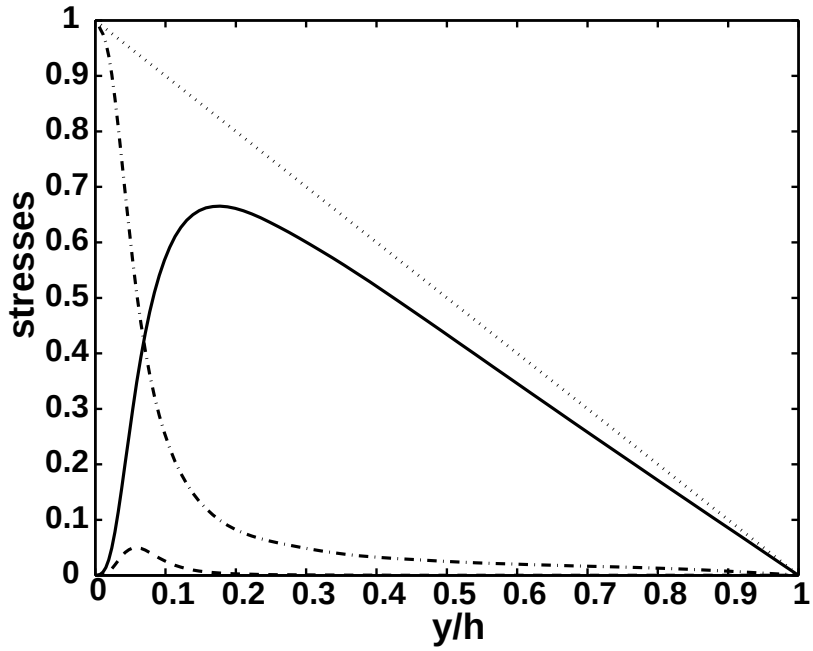

Figure 5.22: Stress components of DES $Re_\tau = 180$: resolved (solid), model (dash), viscous (dashdot) and total (dots).

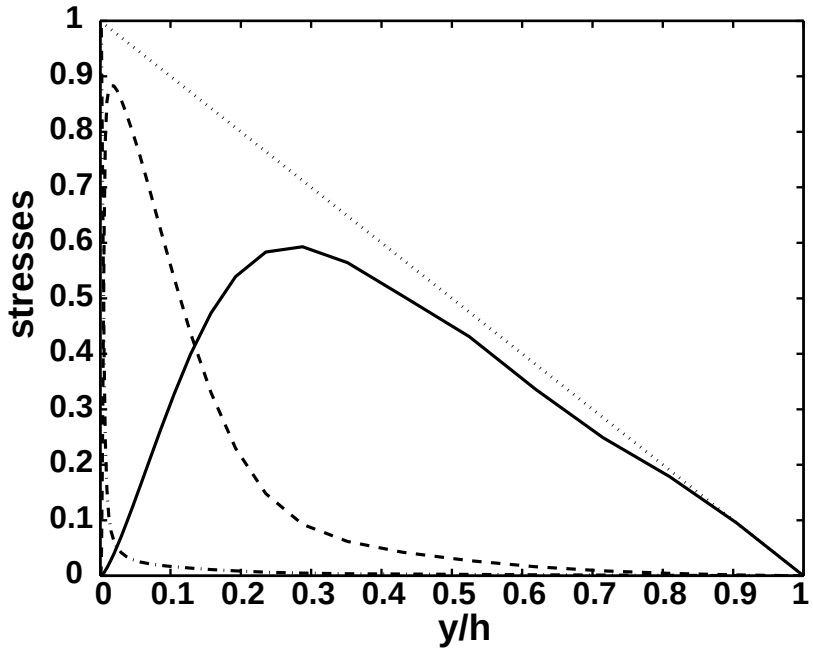

Figure 5.23: Similar to previous figure for DES $Re_\tau = 3000$ case.